Available online at www.sciencedirect.com
ScienceDirect
Journal of Molecular Graphics and Modelling 25 (2006) 549–561
Journal of Molecular Graphics and Modelling
www.elsevier.com/locate/JMGM

Computational prediction of homodimerization of the A_3 adenosine receptor

Soo-Kyung Kim, Kenneth A. Jacobson *

Molecular Recognition Section, Laboratory of Bioorganic Chemistry, National Institute of Diabetes and Digestive and Kidney Diseases (NIDDK), National Institutes of Health (NIH), Bethesda, MD 20892, USA

Received 14 November 2005; received in revised form 13 March 2006; accepted 13 March 2006
Available online 24 March 2006

Abstract

Increasing evidence suggests that G protein-coupled receptors form functional dimers or larger oligomeric complexes through homo- or heterodimerization, and that various transmembrane (TM) domains contribute dimerization interfaces. In this study, monomeric receptor structures – either the monomeric crystallographic structure of bovine rhodopsin or an A_3 adenosine receptor (AR) homology model – were dimerized by computational methods assuming various TM contact regions, optimized, and compared. The semi-empirical oligomeric structure of mouse rhodopsin studied in a native disc membrane with atomic force microscopy was used to establish the distance between monomers in the initial dimeric models. Among eight variations of symmetrical homodimers of bovine rhodopsin, the favored dimeric assembly closely resembled the semi-empirical model, in which TM domains 4 and 5 were the contact site, thus validating this approach. We used similar methods to generate eight homodimers of the A_3AR and found the favored dimeric interface similarly to be TM4–5. By this method, dimeric variations – TM1–2, TM2–3, TM2–4, TM3–4, TM4–5, TM5–6, TM6–7, and TM7–1 – were constructed with the SYBYL 7.0 program by using a novel ''fit-centroids-normal'' method. Fitting atoms considered one of eight TM–TM centroids or seven-TM centroids, two centroids of each monomer, and a normal atom passing through the plane containing all centroids. Following molecular dynamics, the most energetically favorable contact modes were identified. In addition to TM4–5, which was favored in both rhodopsin and A_3AR dimeric models, TM1–2 dimers in which helices 8 also contacted each other were judged favorable. The largest contact surface area between the monomers among the various homodimers, determined by van der Waals calculation with the MOLCAD surface program, was for the TM4–5 dimer. This contact surface also showed a high degree of shape complementarity. In addition, the TM4–5 dimers made by this theoretical method were more stable than the semi-empirically determined dimer.

Keywords: GPCRs; Purine receptors; Rhodopsin; Homology modeling; Protein–protein docking

1. Introduction

G protein-coupled receptors (GPCRs, or seven-transmembrane receptors) are the largest superfamily of proteins in the human body, with more than 1000 different members, and are associated with diverse responses to light, hormones, neurotransmitters, odorants, ions, proteins, and small molecules, including amino acids, nucleotides, and peptides [1,2]. It has been estimated that ~80% of known hormones and neurotransmitters activate cellular signal transduction mechanisms by activating GPCRs [3]. GPCRs represent 30–45% of the current drug targets [4,5]. Most of the 460 nonolfactory GPCRs, the putative first priority for drug targets, belong to family A (the rhodopsin family), which contains 74% of the total GPCR population. In addition, GPCRs, including 150 orphan GPCRs with no known function or selective ligands, have become a major focus in functional genomics programs.

Increasing evidence suggests that GPCRs form functional dimers or larger oligomeric complexes through homodimerization or heterodimerization. Heterodimerization was reported within the same families of GPCRs or between different families of GPCRs or even different receptor superfamilies, such as GPCRs and ligand-gated ion channels [6]. These heteromeric receptors have functional characteristics that differ from homogeneous populations of their constituent receptors, indicating diversity of function among GPCRs [6]. A study of

* Corresponding author at: Molecular Recognition Section, Bldg. 8A, Rm. B1A-19, NIH, NIDDK, LBC, Bethesda, MD 20892-0810, USA.
Tel.: +1 301 496 9024; fax: +1 301 480 8422.
E-mail address: kajacobs@helix.nih.gov (K.A. Jacobson).

1093-3263/$ – see front matter
doi:10.1016/j.jmgm.2006.03.003

the solubilized receptor for leukotriene B_4 (BLT1 receptor) provided strong experimental evidence for a 2:1 stoichiometry of receptor:G protein. In that study, solution-phase neutron-scattering experiments indicated that one heterotrimeric G protein associates with a receptor dimer in the presence of an agonist, suggesting that the active receptor–G protein complex might be a pentamer [7].

Finally, the in situ organization of mouse rhodopsin obtained by atomic force microscopy studies indicates that almost all rhodopsin molecules exist in rows of dimers, with only a few monomers and some single-rhodopsin pairs [8]. A semi-empirical model of the rhodopsin oligomer was released into the Protein Data Bank (PDB; ID: 1N3M) [9]. Dimerization could also affect various stages of the GPCR life cycle. Several studies have shown that dimerization occurs early after biosynthesis and is required for proper transport to the plasma membrane, suggesting that it has a primary role in receptor maturation [10]. The dimeric nature of the receptors has been shown to affect G protein coupling, pharmacological diversity, downstream signaling, and regulatory processes such as internalization [10]. Thus, the concept of dimerization should be considered within the context of screening and development of GPCR-targeted drugs.

Although structural information is required for understanding the mechanism of drug interactions with GPCRs, structure-based drug design with GPCRs was severely restricted because high-resolution structures were not available because of difficulties in expression, purification, and crystallization of GPCRs. However, the availability of the X-ray structure of bovine rhodopsin from the PDB [11] allowed for more structurally directed drug design. (The PDB IDs of rhodopsin crystallized in detergent are 1F88 [12], 1HZX [13], 1L9H [14], and 1GZM [15].) All GPCRs contain common structural components, including seven-transmembrane-spanning α-helical segments connected by alternating intracellular and extracellular loops, with the amino terminus on the extracellular side and the carboxyl terminus on the intracellular side [15]. The high degree of conservation of residues occurs in transmembrane (TM) regions, e.g., a conserved N in TM1, D in TM2, DRY in TM3, W in TM4, P in TM5 and 6, $NPxxY(x)_{5,6}F$ region in TM7, suggesting that these residues are either structurally or functionally important. We have already validated through a rhodopsin-based model those highly conserved residues involved in an intramolecular TM H-bonding [16]. Since the rhodopsin structure serves as a template for the molecular architecture of GPCRs, the recent 3D model of a rhodopsin oligomer by a semi-empirical method could serve as a good template for investigating the dimerization of other GPCRs.

Various studies have suggested that different domains of GPCRs contribute to the dimerization interface. Early studies that carried out co-immunoprecipitation experiments also suggested a crucial role for the carboxyl-terminal tail in the homodimerization of the δ opioid peptide receptor [17]. Data from mutational analysis, individual TM domain expression, and cross-linking experiments suggest that the TM helical domains represent the major dimerization interface in both GPCR homodimers and heterodimers [18]. Several molecular modeling works were also used to predict the corresponding interaction interfaces with bioinformatics. The evolutionary trace method, a data-mining approach for determining significant levels of amino acid conservation, was applied to more than 700 aligned GPCR sequences. The result predicted the occurrence of functionally important clusters of residues on the external faces of TMs 5 and 6 for each family or subfamily of receptors; similar clusters were observed on TMs 2 and 3 [19]. Another computational approach, based on the correlated mutation method, predicted the most frequent GPCR oligomerization interfaces to be specific regions of TMs 4–6 [20,21]. A consideration of all the published data for a variety of GPCRs indicates that most TMs have been proposed to be part of the dimerization interface.

In the present study, the X-ray structure of monomeric rhodopsin was first subjected to a method to predict theoretical dimeric models. The dimers were generated by a novel ''fit-centroids-normal'' method, developed to compare TM interface sites. This method was validated by comparison of the theoretically most stable dimer with the semi-empirical model

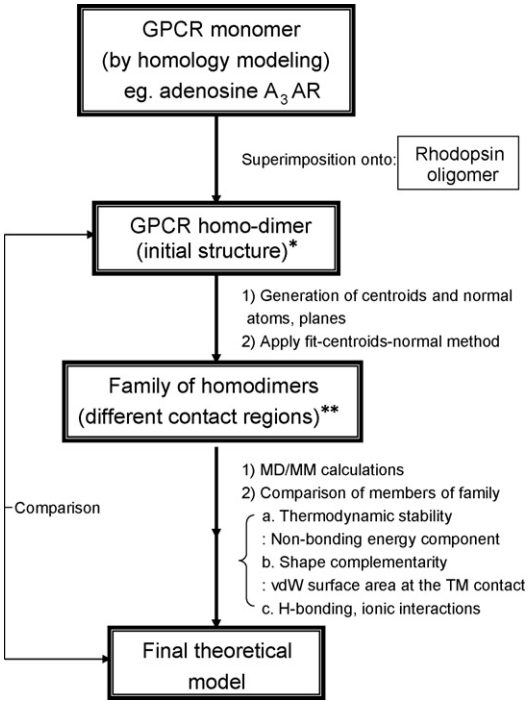

Fig. 1. Flow chart for the generation of eight symmetrical homodimers of rhodopsin and the A_3AR. The X-ray structure of monomeric rhodopsin was first subjected to a method to predict theoretical dimeric models. Following this validation of the method, it was applied to the A_3AR to predict specific homodimeric protein–protein interactions. *To set distance between monomers, the semi-empirical structure of rhodopsin, which was studied in a native disc membrane (PDB ID: 1N3M) with atomic force microscopy [9] and which contains the TMs 4 and 5 as the contact site (4–5′), was used as the initial template. The initial dimer (TM4–5′) of the hA_3AR was created from the theoretical structure of the hA_3AR monomer (PDB ID: 1O74) [23] by using superimposition aligning through structure homology in the Biopolymer module, SYBYL v. 7.0 program. **Various TM contact dimers, TM1–2, TM2–3, TM2–4, TM3–4, TM4–5, TM5–6, TM6–7, and TM7–1, were generated by variation of the contact region and subsequent optimization of the 4–5′ model.

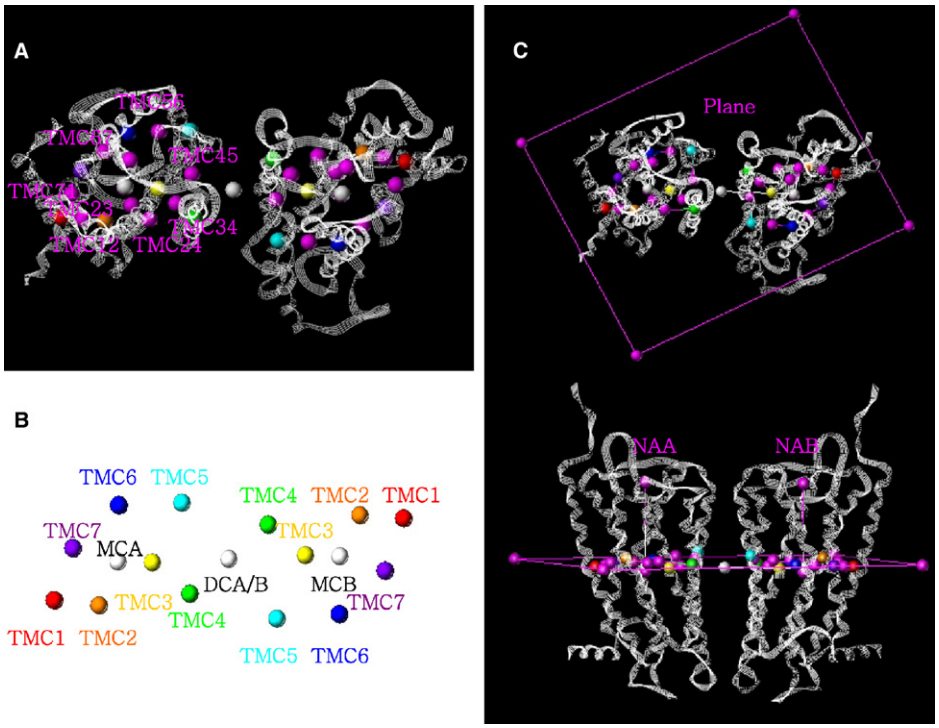

Fig. 2. The A_3AR homodimers from the superimposition onto the rhodopsin template [9]. From the top view, the A_3AR homodimers that display the TM4–5 contact site are represented in a line ribbon model, including all centroids (A). Fitting atoms for the generation of the various contact dimers include (A) the TM–TM centroids ($TMC^{\#\#}$) in magenta, (B) the TM centroids ($TMC^{\#}$) with the same color of each center, the monomer centroids (MCA, MCB), the dimer centroids (DCA, DCB), and (C) the normal atoms (NAA, NAB) passed through the plane in magenta.

of dimeric rhodopsin attained by atomic force microscopy [9]. In addition, adenosine receptors (ARs), being members of the rhodopsin family A GPCRs, were studied for specific homodimeric protein–protein interactions. Several AR subtypes have been shown to form homodimers as well as heterodimers. Although it has not been directly implicated in dimerization, we selected the A_3AR for this study because of the large body of structure–function data about this subtype. While several theoretical studies [19,21] predicted the TM interfaces for dimeric association among rhodopsin family A GPCRs, none of the previous studies generated a set of hypothetical dimeric models and then compared them in stability and shape complementarity.

To predict the contact TM surface area, we generated eight symmetrical homodimer models, for both bovine rhodopsin and the A_3AR. Each model assumed a different TM contact site calculated with the fit-centroids-normal method. All models maintained the same distance between two monomers as in the template, conforming to the semi-empirical model of the atomic force microscopy. To investigate interhelical contact regions, we compared TM1–2, TM2–3, TM2–4, TM3–4, TM4–5, TM5–6, TM6–7, and TM7–1. Fitting atoms shown in Fig. 1 considered the centroid of each of eight TM–TM combinations and the centroid of each seven-TM bundle. Two centroids of each monomer and normal atoms passing through the plane containing all centroids were also included. We found that the TM4–5 dimer showed an energetically favorable homodimer and a high degree of shape complementarity at the TM surface contact area, consistent with the results of atomic force microscopy studies of rhodopsin in the native disc membrane, in which TM4–5 was the contact site.

2. Computational methods

All calculations were performed on a Silicon Graphics (Mountain View, CA) Octane workstation (300 MHz MIPS R12000 [IP30] processor), with the SYBYL 7.0 program [22]. The homology model of the human A_3AR (PDB ID: 1OEA) [23] and the X-ray structure of bovine rhodopsin with 2.8 Å resolution (PDB ID: 1F88) [12] were used for the 3D coordinates of each monomer.

2.1. Generation of homodimers

The overall outline is shown in Fig. 2. The rhodopsin oligomer derived from X-ray crystallography and atomic force microcopy studies (PDB ID: 1N3M) was used as an initial template for the generation of the homodimers from monomers. This superimposition allowed the spacing of the two monomeric units to be the same as in the rhodopsin oligomer, an assumption of our modeling approach. This initial dimer was then subjected to optimization by variation of the contact regions, as described below. Our objective was to apply this process to the A_3AR, but to validate the entire modeling approach we first subjected the rhodopsin monomers to the same process. Each monomer was superimposed onto chains A and C of the rhodopsin dimer, 1N3M, by the align-structure-by-homology command in the SYBYL biopolymer module.

Seven-TM centroids from the backbone atoms of each TM were designated TMC1–7. Eight TM–TM centroids between two TM centroids in the hypothetical dimers were then generated and termed TMC12, TMC23, TMC24, TMC34, TMC45, TMC56, TMC67, and TMC71. Since TM3 is the most internalized of the TMs of rhodopsin and its center is located within the central cavity, hypothetical contact between TM2 and 4 was taken into account. Then, two monomer centroids from all TM centroids (MCA, MCB) and one dimer centroid between two monomer centroids (DCA, DCB) were formed. Finally, normal atoms (NAA, NAB) passing through the plane containing all centroids were created.

In this study, only symmetrical homodimers were considered. The sets of symmetrical homodimers for bovine rhodopsin and the A_3AR were generated assuming TM contact sites TM1–2, TM2–3, TM2–4, TM3–4, TM4–5, TM5–6, TM6–7, and TM7–1, with the fit-centroids-normal method. Fitting atoms included one of eight TM–TM centroids or seven-TM centroids, two monomer centroids, and two normal atoms from each monomer shown in Fig. 1. For example, a TM1–2 contact dimer means TM1 and TM2 in one monomer contact with TM2 and TM1 in the other monomer, respectively. For the generation of the TM dimer, six fitting atoms were used. In the TM1–2 dimer, (1, 2) each TM1 centroid (TMC1), (3, 4) monomer centroid (MCA or MCB) and (5, 6) normal atom (NAA or NAB) of each receptor was fitted into (1′, 2′) the TM4 centroid (TMC4′), (3′, 4′) the monomer centroid (MCA′ or MCB′) and (5′, 6′) the normal atom (NAA′ or NAB′) of the template (the rhodopsin RMSD:0.166, Å the A_3AR RMSD:0.355 Å). In only the TM1–2 contact dimer, helices 8 displayed an additional contact site. Other TM contact dimers were also generated by the same method; (1, 2) each TM or TM–TM centroid in rhodopsin and the A_3AR was superimposed onto (1, 2) TMC3′/4′/5′ or TMC45′ in the template, keeping each monomer centroid and normal atom at the same position.

Table 1 summarizes data for all centroids used in this study and the RMSD value among all six fitting atoms of each molecule. Some TM contact dimers displayed the same TM contact site when different fitting atoms were used. For each TM contact dimer, we selected the best dimer without a bump region at the TM contact site, excluding the loop regions. For example, when generating the TM2–3 dimer, the first fitting atom, TMC23, could be fitted into the template TMC45′ or TM3′. The former dimer displayed bumping at the cytoplasmic ends of each TM1. Thus, the latter dimer without bump regions at the TM interface was selected for the TM2–3 dimer. All homodimers showed the same distance between two monomer centroids and the same tilting angle for the axis of the plane as the template from the semi-empirical model of the atomic force microscopy.

2.2. Molecular dynamics

For the conformational refinement of the various contact dimers of rhodopsin and the A_3AR, the optimized structures were used as a starting point for a subsequent 500-ps molecular dynamics (MD), during which the protein backbone atoms in the secondary structures were constrained. The MD options used were 300 K with a 0.2-ps coupling constant, a time step of 1 fs, and a nonbonded update every 25 fs. The lengths of bonds to hydrogen atoms were constrained according to the SHAKE algorithm [24]. Each average structure from the last 100-ps trajectory of MD was reminimized, at first with backbone constraints in the secondary structure and then without any constraints. The Amber7 FF99 (Force Field) [25] with fixed dielectric constant of 4.0 was used for all calculations, terminating when the conjugate gradient reached 0.05 kcal mol^{-1} $Å^{-1}$.

2.3. Calculation of the van der Waals (vdW) surface area at the TM contact

Mapping of residue polarity and lipophilicity potential [26] to the Connolly surface [27] was carried out with the MOLCAD Molecular Surface program. The vdW surface area at the TM contact of each dimer was calculated by the MOLCAD Separated Surface program [28]. The separating surface is defined by a set of points that are located at the midpoint of the shortest-distance vectors between vdW surface points of the two molecular partners, determined by a grid-based algorithm. The default option, with 1.0 Å grid width and 10.0 Å virtual sphere radii, was used for the generation of vdW surface at the TM contact site. All TM atoms in each monomer were selected for the surface area calculation. The TM contact surface area was computed within an upper bound of 5.0 Å distance from the center of two atoms.

Table 1
Fitting atoms and the RMSD values of eight symmetrical homodimers of bovine rhodopsin and the A_3AR

Contact site	Fitting atoms		RMSD (Å)	
	Homodimer	Template	Rhodopsin	A_3AR
TM1–2	TMC1, MCA/MCB, NAA/NAB	TMC4′, MCA′/MCB′, NAA′/NAB′	0.166	0.355
TM2–3	TMC23, MCA/MCB, NAA/NAB	TMC3′, MCA′/MCB′, NAA′/NAB′	1.034	1.148
TM2–4	TMC24, MCA/MCB, NAA/NAB	TMC45′, MCA′/MCB′, NAA′/NAB′	1.961	1.834
TM3–4	TMC34, MCA/MCB, NAA/NAB	TMC45′, MCA′/MCB′, NAA′/NAB′	1.297	1.099
TM4–5	TMC34, MCA/MCB, NAA/NAB	TMC4′, MCA′/MCB′, NAA′/NAB′	1.636	1.599
TM5–6	TMC56, MCA/MCB, NAA/NAB	TMC4′, MCA′/MCB′, NAA′/NAB′	0.878	1.070
TM6–7	TMC67, MCA/MCB, NAA/NAB	TMC3′, MCA′/MCB′, NAA′/NAB′	0.853	0.533
TM7–1	TMC1, MCA/MCB, NAA/NAB	TMC5′, MCA′/MCB′, NAA′/NAB′	1.158	1.112

3. Results

Computer simulations were performed on the models of various hypothetical, symmetrical contact homodimers built with the X-ray structure of bovine rhodopsin or the homology model of the A_3AR. The fit-centroids-normal method was used to generate eight symmetrical homodimers of bovine rhodopsin and eight similar dimers of the A_3AR. The hypothetical homodimers assumed contact regions of TM1–2, TM2–3, TM2–4, TM3–4, TM4–5, TM5–6, TM6–7, and TM7–1, as explained above (Fig. 3).

At the beginning of the starting geometry, some dimers showed numerous bump regions at the inner loop interface. In rhodopsin and the A_3AR, there were steric collisions at inner loop 2 (IL2) for the TM4–5 contact dimers and at IL3 for the TM5–6 contact dimers. Because of varying conformation and length of the loops, the results for TM7–1 contact dimers of bovine rhodopsin and the A_3AR were very different. The IL2

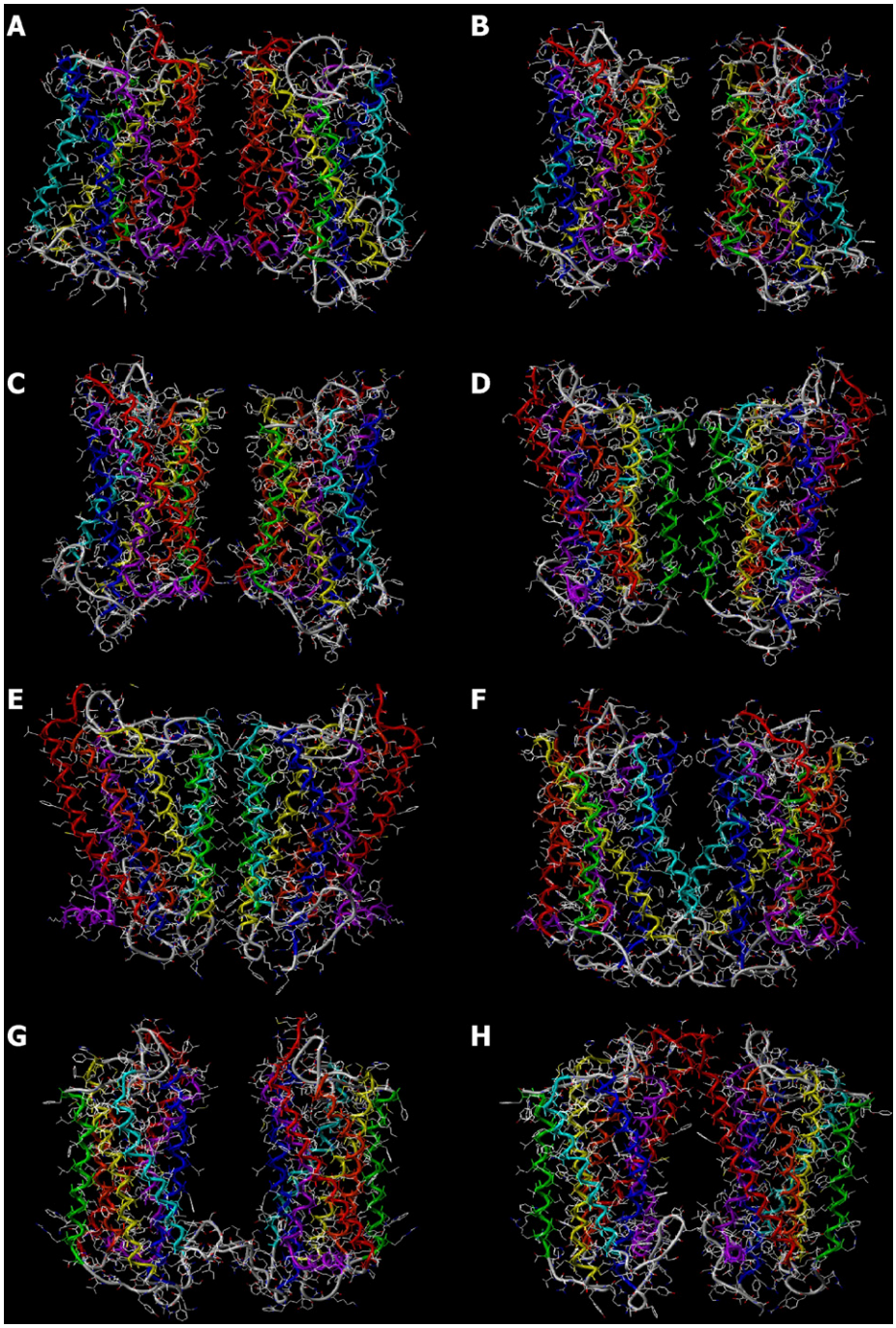

Fig. 3. The various contact dimers of the A_3AR from the MD simulation. (A) TM1–2 contact dimer, (B) TM2–3 contact dimer, (C) TM2–4 contact dimer, (D) TM3–4 contact dimer, (E) TM4–5 contact dimer, (F) TM5–6 contact dimer, (G) TM6–7 contact dimer, and (H) TM7–1 contact dimer. The A_3AR is represented by a tube model of the TMs with seven different colors (TM1 in red, TM2 in orange, TM3 in yellow, TM4 in green, TM5 in cyan, TM6 in blue, and TM7 in purple) and the loops in white from the side view.

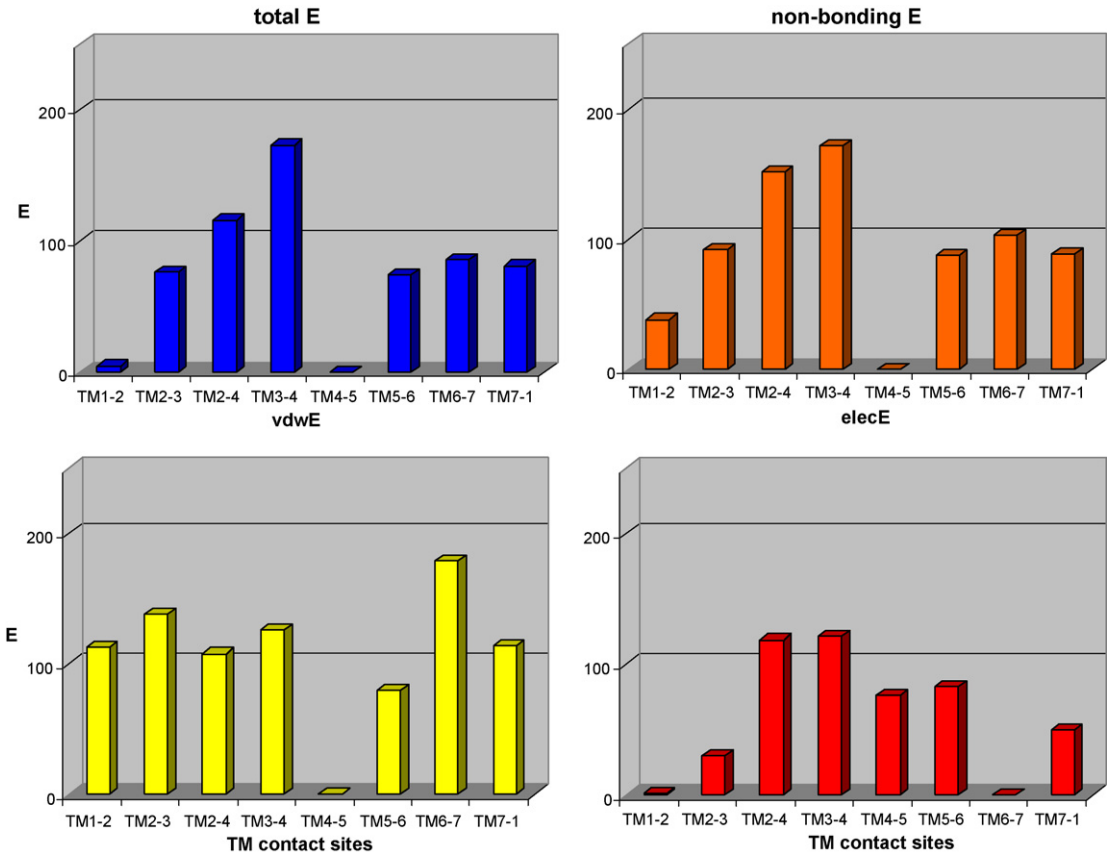

Fig. 4. The relative energy of the rhodopsin dimeric complex with various TM contacts. Each figure shows the total energy, the nonbonding energy, the van der Waals energy, and the electrostatic energy.

and the N/C-terminal region in rhodopsin displayed a steric clash, whereas, the TM7–1 contact dimer of the A_3AR did not show a bump region in any of the loop regions. All bump regions at the inner loop interface between monomers were removed from the 500 ps-MD simulation. However, the rhodopsin TM4–5 and the A_3AR TM5–6 contact dimers, in which one loop intruded into another loop, required a manual correction of the conformation at IL2 and IL3, respectively, before MD simulation.

To eliminate the bump regions at the side chains of the TM interface, 500 ps of MD were performed for all homodimers of rhodopsin and the A_3AR with backbone constraints in the α-helical and β-sheet structures. At the contact area between two monomers, the refinement of the side chains and the removal of a clash area were achieved with short-time MD. The chirality of the Cα atoms and the planarity of the peptide bond were checked to validate the 3D structure of each homodimer.

3.1. The thermal stability of each contact dimer

The thermal stability of each contact dimer was calculated by molecular mechanics (MM) methods according to the relative total energy of each dimeric complex. The MM FF included a bonding and a nonbonding energy component. The nonbonding energy component, including vdW and electrostatic interactions, was highly correlated with the relative total energy of each dimeric complex. The vdW energy was notably a critical component of the thermal stability of the dimeric complex (Fig. 4), suggesting that the major contribution to the energy of each dimeric complex was from the vdW energy at the contact site of each monomer.

In Tables 2 and 3, the relative total energy of hypothetical homodimers of rhodopsin and the A_3AR, assuming various contact sites, is displayed. For each receptor, the dimeric complex displaying the lowest energy was arbitrarily assigned 0 energy. For both sets of rhodopsin and A_3AR homodimers, the TM4–5 contact dimers formed the most energetically favorable dimeric complexes, and the TM1–2 contact dimers with the additional contact region of helix 8 possessed the second-lowest energy. However, there were major differences in thermodynamic stability between these low-energy dimers and other hypothetical dimers with other TM contact regions.

One of the reasons for the low energy of the TM2–4 contact dimer in the A_3AR might be the exclusion of the C-terminal region in the calculation, whereas, in the rhodopsin TM2–4 dimer the C-terminal regions contacted each other, resulting in unfavorable interactions. The TM2–4 and TM3–4 contact dimers of rhodopsin resulted in high energy, while the TM5–6 contact dimer of the A_3AR was the highest-energy complex among the homodimers. A possible explanation for this difference is that IL3 adopted different conformations. The energy of dimeric complexes of the GPCRs was highly dependent on the conformation of the inner loops and the existence of the long C-terminal tails, making it difficult to

Table 2
Summary of the calculation of eight various symmetrical homodimers of bovine rhodopsin

Contact site	Relative complex E (kcal/mol)	TM contact surface area (Å^2)	Intermolecular H-bonding or electrostatic interaction[a]
TM1–2	5	590	Y60(1.55) ↔ T320(H8), T320CO(H8) ↔ T320(H8)
TM2–3	76	36	E150(IL2) ↔ K66(IL1), K339(Cterm) ↔ N151(IL2), K366(Cterm) ↔ E150(IL2)
TM2–4	116	372	E150CO(IL2) ↔ T340(Cterm), T342CO(Cterm) ↔ N145(IL2), Q344CO(Cterm) ↔ R147(IL2)
TM3–4	173	590	R147(IL2) ↔ E150(IL2), N151(IL2) ↔ Y74(2.41)
TM4–5′[b]	248	422	N199(EL2) ↔ N199(EL2), S202(5.37), S144(IL2) ↔ N151(IL2), N145CO(IL2) ↔ H152(4.41), R147(IL2) ↔ S144(IL2)
TM4–5	0	1330	R147CO(IL2) ↔ S144(IL2), N151CO(IL2) ↔ Q225(5.60), N151(IL2) ↔ Y136(3.51), N199(EL2) ↔ S202(5.37)
TM5–6	74	399	E232(IL3) ↔ K248(IL3), E239(IL3) ↔ K231(IL3), R252(6.35) ↔ V227CO(IL3),Y274(6.57) ↔ H278(EL3)
TM6–7	86	0	Q236(IL3) ↔ Q238NH(IL3), S240(IL3) ↔ Q238(IL3)
TM7–1	81	359	E33(Nterm) ↔ K16(Nterm), E33CO(Nterm) ↔ Y30(Nterm), D330(Cterm) ↔ R314(H8), K311(H8)

[a] The numbering in parentheses in the last column followed Ballesteros' numbering convention. Each identifier is composed of a number from 1 to 7 that identifies the helix and, separated by a period, a number associated with a position in that helix. The position number is given relative to the most conserved residues in that helix, which takes the number 50 (N in TM1, D in TM2, R-from DRY-in TM3, W in TM4, and P in TMs 5, 6, and 7).
[b] The TM4–5′ dimer is the template from PDB 1N3M. The relative complex energy was calculated from the MD and the MM optimization. The lowest energy of the dimeric complex was set to zero. The TM contact surface area was calculated by MOLCAD Separated Surface program.

Table 3
Summary of the calculation of eight various symmetrical homodimers of the A_3AR

Contact site	Relative complex E (kcal/mol)	TM contact surface area (Å^2)	Intermolecular H-bonding or electrostatic interaction[a]
TM1–2	5	580	–
TM2–3	45	58	–
TM2–4	0	217	R125(4.40) ↔ K38CO(IL1), L39CO(IL1) ↔ R125(4.40)
TM3–4	26	619	W149(EL2) ↔ M146CO(EL2)
TM4–5′[b]	156	443	W149(EL2) ↔ D175(5.36)
TM4–5	0	1275	R125(4.40) ↔ D199(5.60), T115CO(IL2) ↔ R120(IL2)
TM5–6	330	456	N256(EL3) ↔ E258(EL3), K207(IL3) ↔ S209(IL3)
TM6–7	111	0	–
TM7–1	38	409	–

[a] The numbering in parentheses in the last column followed Ballesteros' numbering convention. Each identifier is composed of a number from 1 to 7 that identifies the helix and, separated by a period, a number associated with a position in that helix. The position number is given relative to the most conserved residues in that helix, which takes the number 50 (N in TM1, D in TM2, R-from DRY-in TM3, W in TM4, and P in TMs 5, 6, and 7).
[b] The TM4–5′ dimer is the template from PDB 1N3M. The relative complex energy was calculated from the MD and the MM optimization. The lowest energy of the dimeric complex was set to zero. The TM contact surface area was calculated using the MOLCAD Separated Surface program.

predict the TM contact site of a GPCR dimer with this parameter alone. In addition, since we performed the short 500 ps level of MD with backbone constraints only for the side-chain refinements, the total energy of dimeric complexes would still depend on the simulation time. However, solely on the basis of the total energy of the dimeric complexes determined here, the theoretical prediction suggesting TM4–5 was the energetically favorable contact site in rhodopsin and the A_3AR was consistent with atomic force microscopy studies that featured a rhodopsin TM4–5 contact dimer [9].

3.2. Structural complementarity of each contact dimer

Structural complementarity is in many cases a major hallmark of a specific protein–protein interaction. In a recent study, 52 out of 75 complexes showed 1600 (±400) Å^2 average area of interface for the recognition site [29]. To complement the use of calculated energies as a criterion for dimerization mode, we also examined the interface region of each hypothetical dimer. To check the level of structural complementarity at the TM interface in the dimeric GPCRs, the Connolly surfaces between two TM monomers were visualized (Fig. 5). The lipophilicity potential of the rhodopsin X-ray structure and the A_3AR homology model projected onto the Connolly surface revealed the characteristics of the membrane proteins. Membrane-spanning regions at the center displayed the most hydrophobicity, while the neutral hydrophilic residues tended to be distributed in the extracellular region. Positively charged hydrophilic residues tended to occur in the intracellular region, consistent with the positive-inside rule for membrane proteins.

For quantitative analysis of the TM contact interface through a MOLCAD Separating Surfaces program (Fig. 6), the vdW surfaces between two monomers at the TM contact area were created and the volumes of the separated surfaces were measured, within an upper bound of 5 Å. The size of the vdW

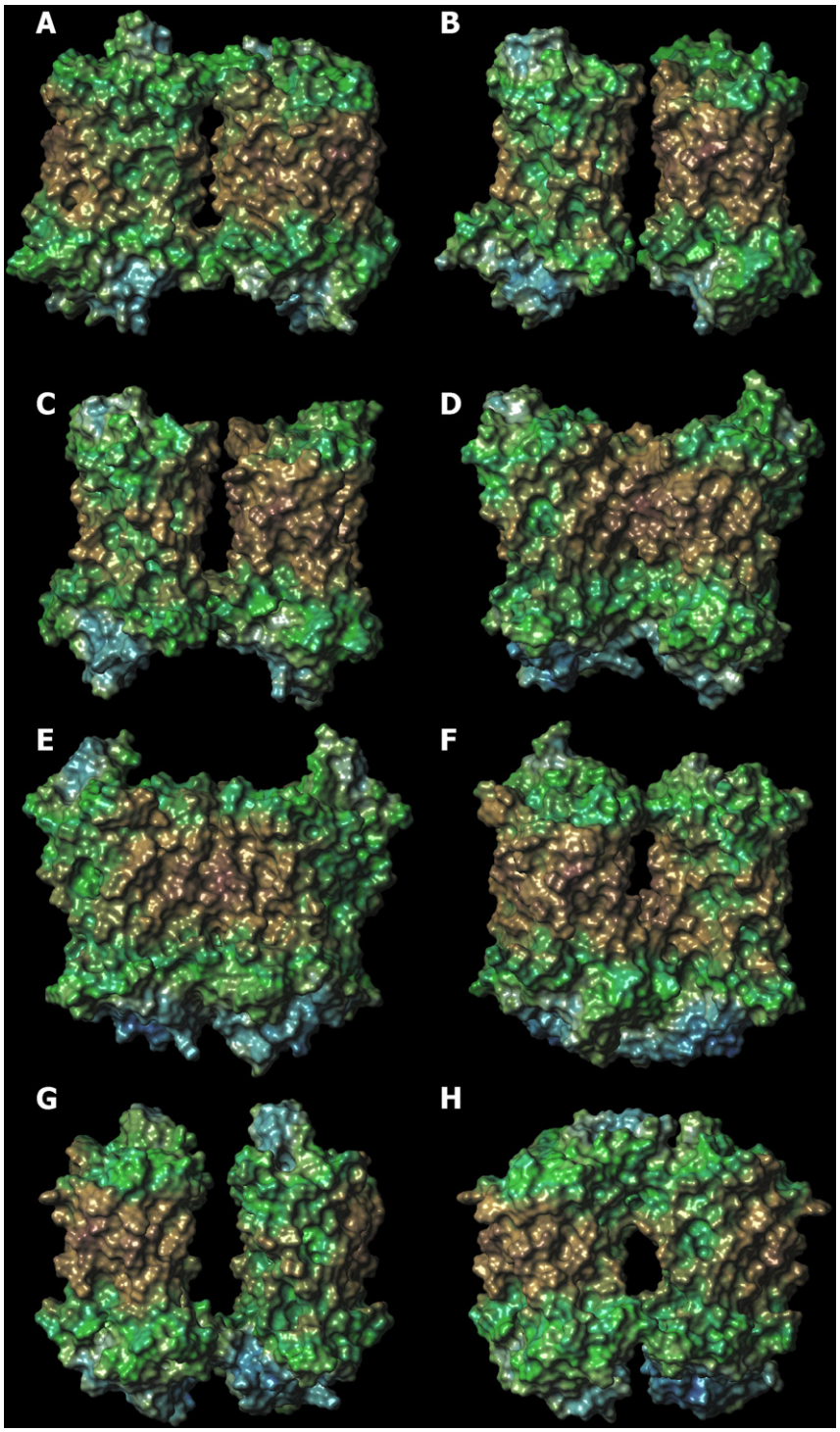

Fig. 5. The Connolly surface with lipophilicity potential in the various contact dimers of the A_3AR from the side view as at the same angle as Fig. 3. The color range for lipophilicity potential ranges from brown (highest lipophilic area of the molecule) to blue (highest hydrophilic area). (A) TM1–2 contact dimer, (B) TM2–3 contact dimer, (C) TM2–4 contact dimer, (D) TM3–4 contact dimer, (E) TM4–5 contact dimer, (F) TM5–6 contact dimer, (G) TM6–7 contact dimer, and (H) TM7–1 contact dimer.

surface characterized the extent of TM contact area overlap for various homodimers. The TM4–5 contact dimers consistently had the most TM contact surface area, with 1330 Å^2 for rhodopsin (Table 2) and 1275 Å^2 for the A_3AR (Table 3). The TM1–2 and TM3–4 contact areas had the next most TM contact surface areas; the same volume with 590 Å^2 for the TM1–2 and TM3–4 dimers in rhodopsin, 580 Å^2 for the TM1–2 contact dimer, and 619 Å^2 for the TM3–4 contact dimer in the A_3AR. The TM2–3 and TM2–4 contact dimers had poor TM contact surface areas. The TM6–7 contact dimer showed no TM contact surface in both cases. Thus, the TM4–5 contact dimers were the dimeric complexes with the best shape complementarity at the

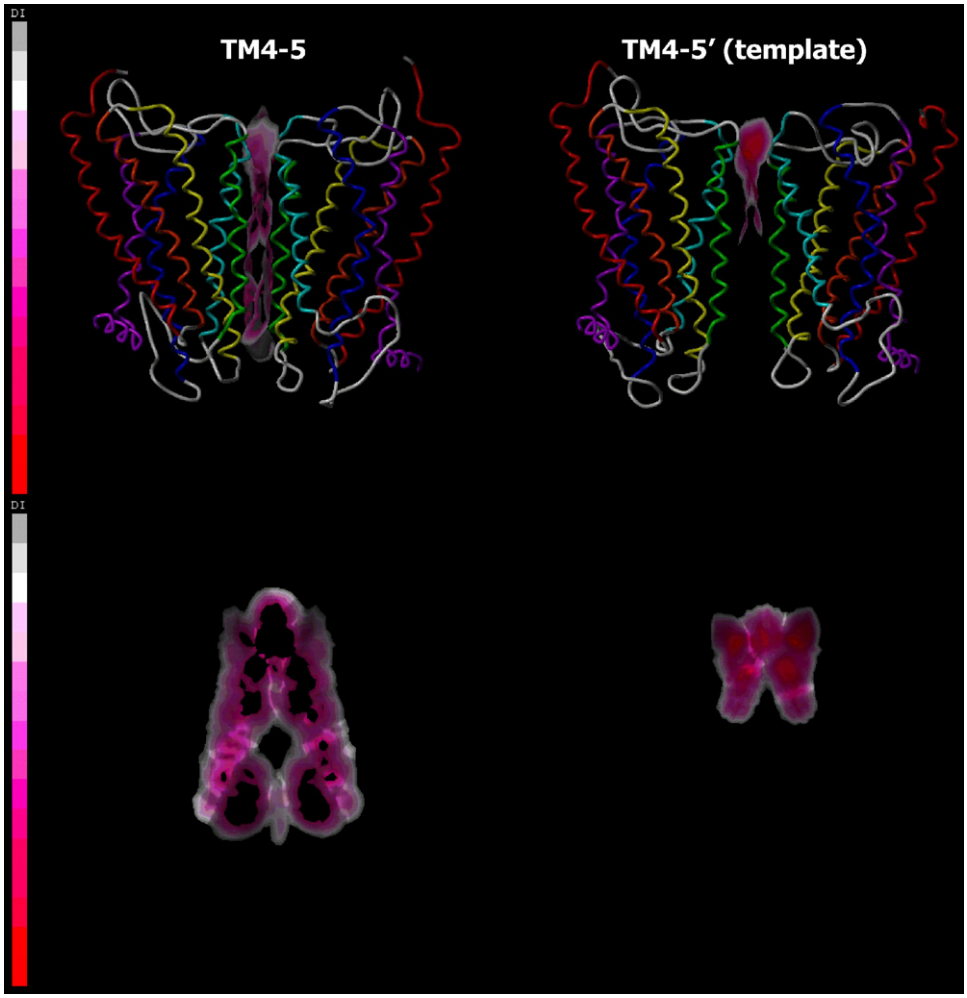

Fig. 6. Comparison of the contact surface complementarity between the rhodopsin TM4–5 contact dimers from the theoretical method on the left side (TM4–5) and the experimental method on the right side (TM4–5′) as a template. The van der Waals contact surfaces at the TM interface were displayed from the side view in the upper figures and from the front view of the contact surface in the lower figures. Distance values from the surface points to the van der Waals surface of the nearest atoms were visualized on the surface as a function of color. The color spectrum ranges from red for the shortest distance to gray for the longest distance. The size of the surface was calculated within a maximum distance of 5 Å.

TM interface, in agreement with the calculation of relative total energy.

3.3. Specific interactions of each contact dimer

Defining favorable protein–protein association principally involves shape matching. However, hydrophobic, H-bonding, and ionic interactions must also be considered [30]. Although the major interactions between the two monomers were hydrophobic, H-bonding and ionic interactions were also detected in the various dimers. In rhodopsin, there are more hydrophilic interactions in the C-terminal region because of the inclusion of the C-terminal tail in the calculation. H-bonding as well as a salt bridge at the TM contact site might be major factors in the formation of homodimerization for GPCRs in general. At the TM4–5 contact region of dimers of rhodopsin (Table 2) and of the A_3AR (Table 3), the most energetically favorable complexes, different hydrophilic interactions indicated that specific interactions would form in the GPCR homodimerization.

3.4. A comparison between the theoretical model and semi-empirical model of atomic force microscopy

Both the theoretical approach in this study and the semi-empirical method of atomic force microscopy featured preferred contact regions consisting of TM4 and TM5, although some differences between the two approaches were evident. There are two possible TM4–5 dimers with different fitting atoms of the TM centroids; one was created by the theoretical approach (TM4–5) and the other was the template from atomic force microscopy (TM4–5′). Notably, the TM4–5 dimer of each receptor made by the theoretical method was considerably more stable than the TM4–5′ dimer generated by the atomic force microscopy (Tables 2 and 3). In addition, the theoretical complex was compatible by the criterion of shape comple-

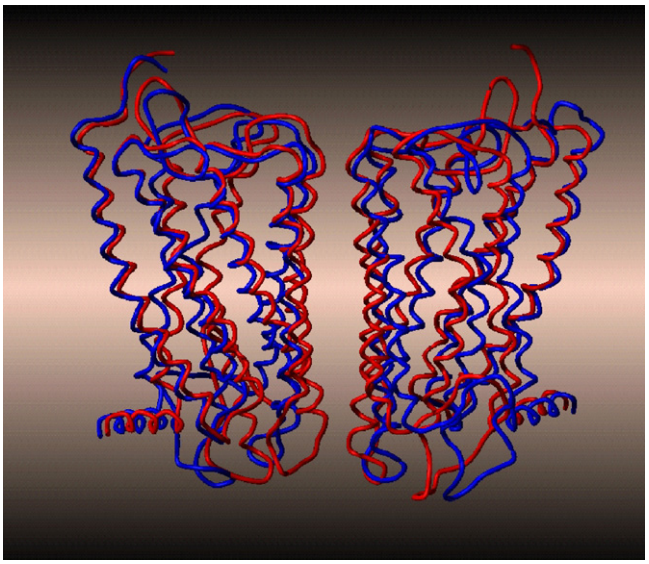

Fig. 7. The superimposition of the TM4–5 contact dimers from the theoretical method in red and the TM4–5′ template from the atomic force microscopy in blue.

mentarity, whereas, the TM4–5′ structure displayed a poor structural match with fewer surface volumes at the cytoplasmic end of the TM interface (Fig. 7). The superimposition of TM4–5 and TM4–5′ dimers shown in Fig. 7 displayed a major difference in the tilting angle of helix 4 at the cytoplasmic end. In the theoretical TM4–5 dimer, the interactions at the TM contact site were maximized, whereas, empty spaces at the lower region of the TM interface existed in the TM4–5′ structure. Thus, the fit-centroids-normal method allows for fine-tuning of the 3D model.

The study of the thermodynamic stability and the shape complementarity of the various contact symmetrical homodimers of rhodopsin and the A_3AR revealed that the TM4–5 contact site is the ideal interface for the homodimerization of the rhodopsin family A GPCRs.

4. Discussion

The existence of GPCR homodimers has been disclosed for the $5HT_{1B}$ and $5HT_{1A}$ serotonin [31,32], D_1 and D_2 dopamine [33,34], A_1 adenosine [35], β_2 adrenergic [36], five metabotropic glutamate [37], muscarinic acetylcholine [38], δ opioid [39], and CCR2 chemokine [40] receptors. Heterodimers composed of different subtypes within the same family have been reported for κ/δ opioid [41], μ/δ opioid [42], $GABA_{B1}$/$GABA_{B2}$ γ-aminobutyric acid [43], M_2/M_3 muscarinic [44], 5-HT_{1B}/5-HT_{1D} serotonin [45], SSTR1/SSTR5 somatostatin [46], SSTR2A/SSTR3 somatostatin [47], and CCR2/CCR5 chemokine [48] receptors. Heterodimerization has also been reported within the same GPCR class for A_1 adenosine/D_1 dopamine [49], A_1 adenosine/$P2Y_1$ nucleotide [50], AT_1 angiotensin/B_2 bradykinin [51], SSTR5 somatostatin/D_2 dopamine [52], β_2 adrenergic/δ opioid [53], β_2 adrenergic/κ opioid [53], between the different GPCR classes for 1α-metabotropic glutamate/A_1 adenosine [54] and five metabotropic glutamate/A_{2A} adenosine [55] receptors, and between members of different receptor superfamilies for D_5 dopamine/ligand-gated $GABA_A$ [56] γ-aminobutyric acid receptors. Thus, the concept of dimerization is important in the development and screening of drugs that act through this GPCR class.

This theoretical work evaluated various hypothetical symmetrical contact homodimers of rhodopsin and the A_3AR to predict a favored dimeric interface. We generated a series of homodimers with the same distance between two monomer TM centers as found in the TM4–5′ structure from the semi-empirical model of atomic force microscopy. The dimers were derived by a novel fit-centroids-normal method and compared by several criteria, including thermal stability, hydropathy, and shape complementarity. The molecular modeling results identified the TM4–5 dimer as an energetically favorable homodimer with a high degree of shape complementarity at the TM surface contact area. The modeling results correlate well with the known experimental results of atomic force microscopy studies of mouse rhodopsin in the native disc membrane under physiological conditions, in which TM4–5 is the contact site. That structure was determined in buffer solution, at room temperature and under normal pressure, without the application of any modification to rhodopsin that may affect its native oligomeric state.

The calculation of the area at TM interfaces gave information on the size of the TM contact area for homodimerization. The TM4–5 dimers, in comparison with other symmetrical homodimers, displayed the optimal TM contact surface because of the surface shape in that region. The TM4–5 contact dimers had a high degree of hydropathy and shape complementarity at the interface. Protein–protein interaction sites have been characterized as flat and solvent accessible, compared with small-molecule binding sites, which are indentations, crevices, or cavities [57]. Thus, considering the tilting of helices, due to the involvement of the straightest helix, i.e., TM4, TM4–5 was the most planar contact site. Thus, by a variety of criteria, TM4–5 is likely to be an ideal interface for family A GPCR homodimerization.

In general, protein homomultimers are more likely than heteromultimers to contain hydrophobic residues at the interface, as revealed from an analysis of six types of protein–protein interfaces [58]. In the context of this study, the fact that the vdW energy is the major contribution to the total energy of the dimeric complexes indicates that mainly hydrophobic residues were present at the TM4–5 contact site.

The TM1–2 contact dimer, in which helix 8 and the C-terminus contacted each other, would be the next most favorable contact site for the formation of an oligomer. The PDB structures of rhodopsin indicated various TM contact sites; however, it was uncertain whether these were truly physiological dimers, because of the existence of detergent in the crystals. The study suggested that detergent interrupts the native oligomeric structure of rhodopsin [59]. The earliest PDB structure of rhodopsin [12] displayed an antiparallel symmetrical dimer with TM1 and helix 8 contact sites; i.e., the cytoplasmic region of one monomer was on the same side as the

extracellular region of the other monomer. In the 2D crystal structure of rhodopsin by Schertler and co-workers [60], molecules form contacts between TM1 and helix 8 and between TM4 and TM5 along the long axis of the unit cell. Parallel dimer formation is mediated partly by interactions between the TM1 of each monomer along with a close interaction between helices 8. However, 2D crystals of squid rhodopsin determined by cryoelectron microscopy display a parallel TM2–4 contact site with interactions mainly at TM4 [61].

Our result indicating that the TM1–2 contact site was the next most energetically favorable supports the possibility of other TM interfaces for oligomerization, consistent with the disulfide-trapping studies of the C5a receptor [62]. Its symmetrical dimer involves an interface between TMs 1 and 2 (TM1–2) or TM 4 (TM4–4); no single dimer model explains all the observed crosslinks, suggesting that C5a receptors form higher-order oligomers. Throughout published studies, the GPCR dimerization in native membrane appears highly dependent on the surrounding environment and/or cell type. The same receptor may function differently within the same cell depending on the cellular environment and the relative density of the receptors [63]. Thus, dimerization of one family of receptors with another can lead to even greater diversity in biological response.

Our direct analysis of the MD results of various symmetrical homodimers revealed significant differences in the thermal stability as well as in the type of intermolecular interactions for various TM contact homodimers of either rhodopsin or the A_3AR, although the lowest (TM4–5) and the second-lowest-energy complexes (TM1–2 and helix 8) were the same for both receptors. Receptor-specific dimerization interfaces likely exist through specific hydrogen bonding as well as electrostatic interactions. The theoretically constructed TM4–5 contact dimers of rhodopsin and the A_3AR had distinct chemical and physical characteristics, all of which may contribute to the receptor-specific interaction.

This method could also be extended to predict GPCR heterodimerization [50], an important subject for further study. GPCR heterodimers have been implicated as a potential disease mechanism, adding a new dimension to rational drug design [6]. One potentially satisfying hypothesis is that multiple non-symmetrical interfaces between TMs contribute to receptor heterodimerization. Since only symmetrical TM interfaces were considered in this study, the possibility of a nonsymmetrical interface between TMs should be examined in further studies. The most likely heterodimerization interfaces of the δ–μ opioid receptor pair involve TM4, TM5, and TM6 of the μ opioid receptor with TM1 of the μ opioid receptor through a subtractive correlated mutation method and the structural information obtained in 3D molecular models of the TM regions of GPCRs built with the rhodopsin crystal structure as a template [21].

Interaction sites between the D_2 and A_{2A}AR are associated with strong functional antagonistic interactions. The rigid-body docking programs ZDOCK 2.1, which uses the shape complementarity score [64], and ESCHER, which determines the shape and electrostatic complementarity by using bump and charge cutoffs [65], found helix 5 and/or 6 and the N-terminal portion of IL3 from the D_2 dopamine receptor in the vicinity of helix 4 and the C-terminal portion of the C-tail from the A_{2A}AR [66]. In particular, compared to homodimerization, the changes in the selectivity of ligand binding and signaling properties that accompany heterodimerization could give rise to an unexpected pharmacological diversity. In addition, the binding of a single agonist to a single receptor might activate neighboring receptors with which the agonist-bound receptor is oligomerized through a transactivation mechanism [6]. These pharmacological diversities could provide new opportunities for the development of more selective compounds that would target specific heterodimers in drug development.

Obviously, the high degree of success we obtained in predicting the TM interface for GPCR homodimerization with our fit-centroids-normal method does not imply that we could predict individual interfaces of all GPCRs at this level of precision. Further experiments are needed to validate a given theoretical model. Through cysteine cross-linking, TM4 was identified as a symmetrical homodimer interface in the dopamine D_2 receptor, a family A GPCR [67]. In a future study of more reliable 3D structures of GPCRs, the use of MD in a fully hydrated lipid bilayer environment will be considered [68]. This bilayer is intended to mimic biological membranes in which lipid molecules interact with TM proteins through many cooperative noncovalent interactions. Nevertheless, our data support the applicability of the present prediction method. Our results should have important implications for delineating methods to infer the TM interface of GPCR homodimerization and heterodimerization.

5. Conclusion

Theoretical models of homodimers of rhodopsin and the A_3AR have been used to investigate experimental evidence suggesting that GPCRs form functional dimers. We examined the thermal stability and shape complementarity of various contact dimers generated by a new theoretical method, the fit-centroid-normal method. The molecular modeling results clearly delineated the TM4–5 interface as leading to an energetically favorable homodimer and a high degree of shape complementarity at the TM surface contact area. These findings correlated well with the semi-empirical model of rhodopsin in the native disc membrane studied by atomic force microscopy. Furthermore, the second most favorable contact dimer at TM1–2, in which helix 8 and the C-terminus contacted each other, would be the next most favorable contact site for oligomer formation. This study offers evidence that dimerization stabilizes GPCRs through hydrophilic as well as hydrophobic interactions with respect to the monomer state. Moreover, this putative model also suggests the possibility of receptor-specific interaction of homodimers.

Acknowledgments

This work was supported by the Intramural Research Program of the NIH, National Institute of Diabetes and Digestive and Kidney Diseases. We thank Dr. Anny Colson and

Dr. Jürgen Wess (NIH/NIDDK, Bethesda, MD) and Dr. David F. Green (Applied Mathematics and Statistics, Stony Brook University, NY) for helpful discussions. We thank Mr. Srikar Rao for proofreading the manuscript.

References

[1] L.F. Kolakowski Jr., GPCRDb: a G protein-coupled receptor database, Receptor Channels 2 (1994) 1–7.
[2] U. Gether, Uncovering molecular mechanisms involved in activation of G protein-coupled receptors, Endocr. Rev. 21 (2000) 90–113.
[3] L. Birnbaumer, J. Abramowitz, A.M. Brown, Receptor-effector coupling by G proteins, Biochem. Biophys. Acta 1031 (1990) 163–224.
[4] J. Drews, Drug discovery: a historical perspective, Science 287 (2000) 1960–1964.
[5] A.L. Hopkins, C.R. Groom, The druggable genome, Nat. Rev. Drug. Discov. 1 (2002) 727–730.
[6] S.R. George, B.F. O'Dowd, S.P. Lee, G-protein-coupled receptor oligomerization and its potential for drug discovery, Nat. Rev. Drug Discov. 1 (2002) 808–820.
[7] J.-L. Baneres, J. Parello, Structure-based analysis of GPCR function: evidence for a novel pentameric assembly between the dimeric leukotriene B_4 receptor BLT1 and the G-protein, J. Mol. Biol. 329 (2003) 815–829.
[8] D. Fortiadis, Y. Liang, S. Filipek, D.A. Saperstein, A. Engel, K. Palczewski, Atomic-force microscopy: rhodopsin dimers in native disc membranes, Nature 421 (2003) 127–128.
[9] Y. Liang, D. Fortiadis, S. Filipek, D.A. Saperstein, K. Palczewski, A. Engel, Organization of the G protein-coupled receptors rhodopsin and opsin in native membranes, J. Biol. Chem. 278 (2003) 21655–21662.
[10] S. Terrillon, M. Bouvier, Roles of G-protein-coupled receptor dimerization; from ontogeny to signaling regulation, EMBO Rep. 5 (2004) 30–34.
[11] H.M. Berman, J. Westbrook, Z. Feng, G. Gilliland, T.N. Bhat, H. Weissig, I.N. Shindyalov, P.E. Bourne, The protein data bank, Nucl. Acids Res. 28 (2000) 235–242.
[12] K. Palczewski, T. Kumasaka, T. Hori, C.A. Behnke, H. Motoshima, Crystal structure of rhodopsin: a G protein-coupled receptor, Science 289 (2000) 739–745.
[13] D.C. Teller, T. Okada, C.A. Behnke, K. Palczewski, R.E. Stenkamp, Advances in determination of a high-resolution three-dimensional structure of rhodopsin, a model of G-protein-coupled receptors (GPCRs), Biochemical 40 (2001) 7761–7762.
[14] T. Okada, Y. Fujiyoshi, M. Silow, J. Navarro, E.M. Landau, Y. Shichida, Fundamental role of internal water molecules in rhodopsin revealed by X-ray crystallography, Proc. Natl. Acad. Sci. U.S.A. 99 (2002) 5982–5987.
[15] J. Li, P.C. Edwards, M. Burghammer, C. Villa, G.F.X. Schertler, Structure of bovine rhodopsin in a trigonal crystal form, J. Mol. Biol. 343 (2004) 1409–1438.
[16] S.-K. Kim, Z.-G. Gao, P. van Rompaey, A.S. Gross, A. Chen, S. van Calenbergh, K.A. Jacobson, Modeling the adenosine receptors: comparison of the binding domains of A_{2A} agonists and antagonists, J. Med. Chem. 46 (2003) 4847–4859.
[17] S. Cvejic, L.A. Devi, Dimerization of the delta opioid receptor: implication for a role in receptor internalization, J. Biol. Chem. 272 (1997) 26959–26964.
[18] S. Bulenger, S. Marullo, M. Bouvier, Emerging role of homo- and heterodimerization in G-protein-coupled receptor biosynthesis and maturation, Trends Pharmacol. Sci. 26 (2005) 131–137.
[19] M.K. Dean, C. Higgs, R.E. Smith, R.P. Bywater, C.R. Snell, P.D. Scott, G.J. Upton, T.J. Howe, C.A. Reynolds, Dimerization of G-protein-coupled receptors, J. Med. Chem. 44 (2001) 4595–4614.
[20] M. Filizola, H. Weinstein, The study of G-protein coupled receptor oligomerization with computational modeling and bioinformatics, FEBS J. 272 (2005) 2926–2938.
[21] M. Filizola, O. Olmea, H. Weinstein, Prediction of heterodimerization interfaces of G-protein coupled receptors with a new subtractive correlated mutation method, Protein Eng. 15 (2002) 881–885.
[22] SYBYL®, version 7.0, 1699, Tripos Inc., South Hanley, St. Louis, Missouri 63144.
[23] Z.-G. Gao, S.-K. Kim, T. Biadatti, W. Chen, K. Lee, D. Barak, S.G. Kim, C.R. Johnson, K.A. Jacobson, Structural determinants of A_3 adenosine receptor activation: nucleoside ligands at the agonist/antagonist boundary, J. Med. Chem. 45 (2002) 4471–4484.
[24] J.P. Ryckaert, G. Ciccotti, H.J.C. Berendsen, Numerical integration of the Cartesian equations of motion for a system with constraints: molecular dynamics of *n*-alkanes, J. Comput. Phys. 23 (1977) 327–341.
[25] D.A. Case, T.E. Cheatham III, T. Darden, H. Gohlke, R. Luo, K.M. Merz Jr., A. Onufriev, C. Simmerling, B. Wang, R.J. Woods, The Amber biomolecular simulation programs, J. Comput. Chem. 26 (2005) 1668–1688.
[26] W. Heiden, G. Moeckel, J. Brickmann, A new approach to the display of local lipophilicity/hydrophilicity mapped on molecular surfaces, J. Comput. Aided Mol. Design. 7 (1993) 503–514.
[27] M.L. Connolly, Solvent-accessible surfaces of proteins and nucleic acids, Science 221 (1983) 709–713.
[28] M. Keil, T.E. Exner, J. Brickmann, Characterization of protein–ligand interfaces: separating surfaces, J. Mol. Mod. 4 (1998) 335–339.
[29] L. Lo Conte, C. Chothia, J. Janin, The atomic structure of protein–protein recognition sites, J. Mol. Biol. 285 (1999) 2177–2198.
[30] A.H. Elcock, D. Sept, J.A. McCammon, Computer simulation of protein–protein interactions, J. Phys. Chem. B 105 (2001) 1504–1518.
[31] G.Y. Ng, S.R. George, R.L. Zastawny, M. Caron, M. Bouvier, M. Dennis, B.F. O'Dowd, Human $Serotonin_{1B}$ receptor expression in Sf9 cells: phosphorylation, palmitoylation, and adenylyl cyclase inhibition, Biochemical 32 (1993) 11727–11733.
[32] P.J. Pauwels, D.S. Dupuis, M. Perez, S. Halazy, Dimerization of 8-OH-DPAT increases activity at serotonin 5-HT_{1A} receptors, Naunyn Schmiedeberg's Arch. Pharmacol. 358 (1998) 404–410.
[33] G.Y. Ng, B. Mouillac, S.R. George, M. Caron, M. Dennis, M. Bouvier, B.F. O'Dowd, Desensitization, phosphorylation and palmitoylation of the human dopamine D_1 receptor, Eur. J. Pharmacol. 267 (1994) 7–19.
[34] G.Y. Ng, B.F. O'Dowd, M. Caron, M. Dennis, M.R. Brann, S.R. George, Phosphorylation and palmitolylation of the human D2L domain receptor in Sf9 cells, J. Neurochem. 63 (1994) 1589–1595.
[35] F. Ciruela, V. Casadó, J. Mallol, E.I. Canela, C. Lluis, R. Franco, Immunological identification of A_1 adenosine receptors in brain cortex, J. Neurosci. Res. 42 (1995) 818–828.
[36] T.E. Herbert, S. Moffett, J.P. Morello, T.P. Loise, D.G. Bichet, C. Barret, M. Bouvier, A peptide derived from a beta2-adrenergic receptor transmembrane domain inhibits both receptor dimerization and activation, J. Biol. Chem. 271 (1996) 16384–16392.
[37] C. Romano, W.L. Yang, K.L. O'Malley, Metabotropic glutamate receptor 5 is a disulfide-linked dimer, J. Biol. Chem. 271 (1996) 28612–28616.
[38] R. Maggio, P. Barbier, F. Fornai, G.U. Corsini, Functional role of the third cytoplasmatic loop in muscarinic receptor dimerization, J. Biol. Chem. 271 (1996) 31055–31060.
[39] S. Cvejic, L.A. Devi, Dimerization of the delta opioid receptor: implication for a role in receptor internalization, J. Biol. Chem. 272 (1997) 26959–26964.
[40] J.M. Rodriguez-Frade, A.J. Vila-Coro, A. Martin, J.P. Albar, C. Martinez, M. Mellado, The chemokine monocyte chemoattractant protein-1 induces functional responses through dimerization of its receptor CCR2, Proc. Natl. Acad. Sci. 96 (1999) 3628–3633.
[41] B.A. Jordan, L.A. Devi, G protein-coupled receptor heterodimerization modulates receptor function, Nature 399 (1999) 697–700.
[42] S.R. George, T. Fan, Z. Xie, R. Tse, V. Tam, G. Varghese, B.F. O'Dowd, Oligomerization of μ- and δ-opioid receptors. Generation of novel functional properties, J. Biol. Chem. 275 (2000) 26128–26135.
[43] K.A. Jones, B. Borowsky, J.A. Tamm, D.A. Craig, M.M. Durkin, M. Dai, W.J. Yao, M. Johnson, C. Gunwaldsen, L.Y. Huang, C. Tang, Q. Shen, J.A. Salon, K. Morse, T. Laz, K.E. Smith, D. Nagarathnam, S.A. Noble, T.A. Branchek, C. Gerald, $GABA_B$ receptors function as a heteromeric assembly of the subunits $GABA_B$ R1 and $GABA_B$ R2, Nature 396 (1999) 674–679.
[44] R. Maggio, P. Barbier, A. Colelli, F. Salvadori, G. Demontis, G.U. Corsini, G protein-linked receptors: pharmacological evidence for the formation of heterodimers, J. Pharmacol. Exp. Ther. 291 (1999) 251–257.

[45] Z. Xie, S.P. Lee, B.F. O'Dowd, S.R. George, Serotonin 5-HT_{1B} and 5-HT_{1D} receptors form homodimers when expressed alone and heterodimers when co-expressed, FEBS Lett. 456 (1999) 63–67.
[46] M. Rocheville, D.C. Lange, U. Kumar, R. Sasi, R.C. Patel, Y.C. Patel, Subtypes of the somatostatin receptor assemble as functional homo- and heterodimers, J. Biol. Chem. 275 (2000) 7862–7869.
[47] M. Pfeiffer, T. Koch, H. Schroder, M. Klutzny, S. Kirscht, H.J. Kreienkamp, V. Hollt, S. Schulz, Homo- and heterodimerization of somatostatin receptor subtypes. Inactivation of sst(3) receptor function by heterodimerization with sst(2A), J. Biol. Chem. 276 (2001) 14027–14036.
[48] M. Mellado, J.M. Rodriquez-Frade, A.J. Vila-Coro, S. Fernandez, de Ana A. Martin, D.R. Jones, J.L. Toran, C. Martinez-A, Chemokine receptor homo- or heterodimerization activates distinct signaling pathways, EMBO J. 20 (2001) 2497–2507.
[49] S. Ginés, J. Hillion, M. Torvinen, S. Le Crom, V. Casado, E.I. Canela, S. Rondin, J.Y. Lew, S. Watson, M. Zoli, L. Agnati, P. Vernier, C. Lluis, S. Ferré, K. Fuxe, R. Franco, Dopamine, D_1 and adenosine A_1 receptors assemble into functionally interacting heteromeric complexes, Proc. Natl. Acad. Sci. U.S.A. 97 (2000) 8606–8611.
[50] K. Yoshioka, O. Saitoh, H. Nakata, Heteromeric association creates a P2Y-like adenosine receptor, Proc. Natl. Acad. Sci. U.S.A. 98 (2001) 7617–7622.
[51] S. AbdAlla, H. Lother, U. Quitterer, AT_1-receptor heterodimers show enhanced G-protein activation and altered receptor sequestration, Nature 407 (2000) 94–98.
[52] M. Rocheville, D.C. Lange, U. Kumar, S.C. Patel, R.C. Patel, Y.C. Patel, Receptors for dopamine and somatostatin: formation of hetero-oligomers with enhanced functional activity, Science 288 (2000) 154–157.
[53] B.A. Jordan, N. Trapaidze, I. Gomes, R. Nivarthi, L.A. Devi, Oligomerization of opioid receptors with β_2-adrenergic receptors: a role in trafficking and mitogen-activated protein kinase activation, Proc. Natl. Acad. Sci. U.S.A. 98 (2001) 343–348.
[54] F. Ciruela, M. Escriche, J. Burgueno, E. Angulo, V. Casado, M.M. Soloviev, E.I. Canela, J. Mallol, W.Y. Chan, C. Lluis, R.A. McIlhinney, R. Franco, Metabotropic glutamate 1alpha and adenosine A_1 receptors assemble into functionally interacting complexes, J. Biol. Chem. 276 (2001) 18345–18351.
[55] S. Ferré, M. Karcz-Kubicha, B.T. Hope, P. Popoli, J. Burgueno, M.A. Gutiérrez, V. Casado, K. Fuxe, S.R. Goldberg, C. Lluis, R. Franco, F. Ciruela, Synergistic interaction between adenosine A_{2A} and glutamate mGlu5 receptors: Implications for striatal neuronal function, Proc. Natl. Acad. Sci. U.S.A. 99 (2002) 11940–11945.
[56] F. Liu, Q. Wang, Z.B. Pristupa, X.M. Yu, Y.T. Wang, H.B. Niznik, Direct protein–protein coupling enables crosstalk between dopamine D_5 and gamma-aminobutyric $acid_A$ receptors, Nature 403 (2000) 274–280.
[57] S. Jones, J.M. Thornton, Analysis of protein–protein interaction sites using surface patches, J. Mol. Biol. 272 (1997) 121–132.
[58] Y. Ofran, B. Rost, Analysing six types of protein–protein interfaces, J. Mol. Biol. 325 (2003) 377–387.
[59] D. Fortiadis, Y. Liang, S. Filipek, D.A. Saperstein, A. Engel, K. Palczewski, The G protein-coupled receptor rhodopsin in the native membrane, FEBS Lett. 421 (2004) 281–288.
[60] J.J. Ruprecht, T. Mielke, R. Vogel, C. Villa, G.F.X. Schertler, Electron crystallography reveals the structure of metarhodopsin I, EMBO J. 23 (2004) 3609–3620.
[61] A. Davies, B.E. Gowen, A.M. Krebs, G.F.X. Schertler, H.R. Saibil, Three-dimensional structure of an invertebrate rhodopsin and basis for ordered alignment in the photoreceptor membrane, J. Mol. Biol. 314 (2001) 455–463.
[62] J.M. Klco, T.B. Lassere, T.J. Baranski, C5a receptor oligomerization. I. Disulfide trapping reveals oligomers and potential contact surfaces in a G protein-coupled receptor, J. Biol. Chem. 278 (2003) 35345–35353.
[63] J. Tallman, Dimerization of G-protein-coupled receptors: implications for drug design and signaling, Neuropsychopharmacology 23 (2000) S1–S2.
[64] R. Chen, L. Li, Z. Weng, ZDOCK: an initial-stage protein-docking algorithm, Proteins 52 (2003) 80–87.
[65] G. Ausiello, G. Cesareni, M. Helmer-Citterich, ESCHER: a new docking procedure applied to the reconstruction of protein tertiary structure, Proteins 28 (1997) 556–567.
[66] M. Canals, D. Marcellino, F. Fanelli, F. Ciruela, P. de Benedetti, S.R. Goldberg, K. Neve, K. Fuxe, L.F. Agnati, A.S. Woods, S. Ferré, C. Lluis, M. Bouvier, R. Franco, Adenosine A_{2A}-dopamine D_2 receptor–receptor heteromerization. Qualitative and quantitative assessment by fluorescence and bioluminescence energy transfer, J. Biol. Chem. 278 (2003) 46741–46749.
[67] W. Guo, L. Shi, J.A. Javitch, The fourth transmembrane segment forms the interface of the dopamine D_2 receptor homodimer, J. Biol. Chem. 278 (2003) 4385–4388.
[68] T.B. Woolf, B. Roux, Molecular dynamics simulation of the gramicidin channel in a phopholipid bilayer, Proc. Natl. Acad. Sci. U.S.A. 91 (1994) 11631–11635.